Biosensors and Bioelectronics 287 (2025) 117725

Contents lists available at ScienceDirect

Biosensors and Bioelectronics

journal homepage: www.elsevier.com/locate/bios

Multiplexed and streamlined DNA methylation detection of colorectal cancer-related genes using graphically encoded hydrogel microparticles and rolling circle amplification

Wookyoung Jang [a,1], So Jung Oh [a,1], Eun Sun Kim [b,*], Ki Wan Bong [a,**]

[a] Department of Chemical and Biological Engineering, Korea University, Seoul, 02841, Republic of Korea
[b] Department of Gastroenterology, Korea University College of Medicine, Seoul, 02841, Republic of Korea

ARTICLE INFO

Keywords:
DNA methylation
Multiplex detection
Hydrogel
Microparticle
Rolling circle amplification
Colorectal cancer

ABSTRACT

Detection of DNA methylation in multiple genes can contribute to the prediction, diagnosis, and prognosis of diverse diseases. However, current DNA methylation detection technologies, such as PCR and microarrays, suffer from limited multiplexing capabilities or complicated assay procedures that require pre-amplification. To circumvent these limitations, we present a graphically encoded hydrogel microparticle-based multiplexed DNA methylation process mediated by rolling circle amplification (RCA) for signal enhancement. Unlike typical DNA methylation detection technologies, the developed process does not depend on pre-amplification and has a large multiplexing capacity based on graphic-based encoding. By the streamlined integration of bisulfite-based sequence conversion, ligation of padlock DNA, and hydrogel-based RCA, colorectal cancer-related genes (VIM and SDC2) can be detected with sensitivities of 23.3 fM and 54.1 fM. Furthermore, methylated DNA in a mixture of methylated and unmethylated DNA can be differentiated at levels as low as 0.1 %. The robust multiplexing capability of VIM and SDC2 was also confirmed by the negligible non-specific signal and consistency of the detection signal with the singleplex assay (81.9 % and 94.7 % recovery rates for VIM and SDC2, respectively). Finally, the practical applicability of the assay was validated by analyzing the methylation levels of VIM and SDC2 in cellular DNA extracted from normal and colorectal cancer cell lines. Given its multiplexing capability, streamlined workflow, robust sensitivity, and specificity, the developed assay can contribute to various biomedical and omics fields, including cancer diagnosis.

1. Introduction

DNA methylation, a representative epigenetic hallmark (Suzuki and Bird, 2008), indicates the addition of methyl groups to cytosines in CpG islands of genomic DNA. Numerous studies have revealed that the methylation levels of specific gene sequences in the genome are highly related to the occurrence and progression of various diseases (Jin and Liu, 2018). Therefore, DNA methylation can be an efficient biomarker for the prediction, diagnosis, and prognosis of diverse diseases, such as cancer (Liang et al., 2021; Zhao et al., 2023), Alzheimer's disease (Weng et al., 2013), and rheumatoid arthritis (Ballestar et al., 2020). In particular, DNA methylation analysis has emerged as a next-generation early diagnostic tool for cancer based on 1) the high epigenetic correlation with the onset of cancers and 2) the capability of non-invasive analysis of biological samples, such as blood, urine, and stool (Chen et al., 2019a, 2020; Yu et al., 2024). For instance, methylation analysis of the syndecan 2 (SDC2) gene in stool DNA has been widely utilized in clinical fields to diagnose colorectal cancer, including early stage cases (Han et al., 2019; Zhang et al., 2024). Although several biomarkers, including microRNAs, have been investigated for cancer diagnosis (Al Sulaiman et al., 2022), DNA methylation can contribute to the early diagnosis of cancers in terms of both sensitivity and specificity through specific indicators of gene expression patterns. For example, while diverse microRNAs are involved in multiple molecular pathways (Bautista-Sánchez et al., 2020), DNA methylation can reveal the dysregulated expression of specific genes in the genome.

* Corresponding author.
** Corresponding author.
E-mail addresses: silverkes@naver.com (E.S. Kim), bong98@korea.ac.kr (K.W. Bong).
[1] These authors contributed equally to this work.

https://doi.org/10.1016/j.bios.2025.117725
Received 6 April 2025; Received in revised form 17 June 2025; Accepted 21 June 2025
Available online 27 June 2025

Polymerase chain reaction (PCR)-based detection technologies have mostly been utilized to analyze DNA methylation because of their superior sensitivity based on the exponential target amplification process (Wani and Aldape, 2016). In particular, the integration of bisulfite treatment-based sequence conversion with PCR has been widely used (Jiang et al., 2010; Wani and Aldape, 2016). Unmethylated cytosine in genomic DNA can be converted to uracil by bisulfite treatment, whereas methylated cytosine remains intact. Therefore, with the proper design of primers targeting methylated genomic regions, methylated genes can be specifically amplified by PCR following bisulfite treatment. However, PCR-based DNA methylation analysis techniques are limited when implementing multiplex detection processes. Simultaneous methylation analysis of multiple genes through multiplexed detection is highly advantageous because of low sample consumption and enhanced diagnostic accuracy. In particular, multiplexed DNA methylation analysis can lead to the simultaneous diagnosis of multiple cancers by the comprehensive analysis of individual genes specific to each cancer type. However, because typical multiplex PCR technologies use multiple fluorescent dyes to encode each target analyte, the number of detectable targets in multiplex assays is limited (fewer than five targets) owing to the overlapping of fluorescence spectra (Jet et al., 2021). Although sequencing approaches for PCR amplicons can be exploited to enhance the capability of multiplexing, they also have limitations, such as the long duration of target hybridization and the requirement for expensive and sophisticated equipment (Gong et al., 2022). Furthermore, there is a vulnerability related to false-positive signal expression due to non-specific cross-talk between the target and primer in multiplex PCR (Healy et al., 2021; Li et al., 2005). Although several isothermal amplification techniques, such as rolling circle amplification (RCA), have been utilized for DNA methylation detection, these assays have normally been constrained to detecting a single target in a single sample because of a lack of multiplexing capability (Wang et al., 2022; Zhang et al., 2025).

To overcome the limitations of PCR-based DNA methylation analysis in terms of multiplexing, microarray techniques can be an alternative, as they can detect more than a few hundred analytes in a single sample (Bibikova et al., 2011; Heiss and Just, 2018; Schumacher et al., 2006; Zhao et al., 2023). Compared to planar microarrays, suspension microarrays have distinct advantages, including high assay sensitivity and short assay time, which are attributed to their superior reaction kinetics in the suspension phase (Birtwell and Morgan, 2009). Accordingly, several suspension microarray techniques have been developed to analyze DNA methylation in a multiplexed manner, leading to the diagnosis of various diseases, including cancer (Bibikova et al., 2006; Zhao et al., 2023). However, despite their high multiplexing capability, microarray platforms normally require pre-amplification steps for target analytes, such as PCR, with limited sensitivity, which makes the overall assay time-consuming and labor-intensive. In addition, the pre-amplification step can increase vulnerability to carryover contamination and off-target amplification (Li et al., 2023a, 2023b). Therefore, the development of a streamlined and sensitive suspension microarray technology for DNA methylation without any pre-amplification procedures is in high demand.

Recently, suspension-microarray-based sensitive bioassays have been developed using signal amplification strategies, such as RCA and hybridization chain reaction (HCR) (Jang et al., 2024; Kim et al., 2021; Mun et al., 2023). These signal amplification strategies enable the labeling of multiple fluorophores on a single target captured by microparticles. Therefore, a high detection signal can be achieved even for trace amounts of the target analytes, leading to an enhanced sensitivity of more than one order of magnitude. Furthermore, the sequential integration of signal amplification techniques with conventional suspension microarray-based bioassays enables streamlining of the overall assay while concurrently reducing vulnerability to off-target amplification compared to the target amplification process. RCA has frequently been used as a signal amplification technique for suspension microarrays because of its high reaction kinetics and superior specificity (Al Sulaiman et al., 2022; Mun et al., 2023; Wu et al., 2022). However, even though diverse target analytes, such as proteins, single nucleotide polymorphisms (SNPs), and microRNAs, have been detected with signal amplification-based suspension microarray techniques (Al Sulaiman et al., 2022; Jang et al., 2024; Mun et al., 2023), studies addressing DNA methylation were lacking until recently.

Graphically encoded hydrogel microparticle is a powerful suspension microarray platform for diverse types of target analytes, such as proteins (Jang et al., 2024), microRNAs (Al Sulaiman et al., 2022), and DNA (Choi et al., 2022). The graphical codes of the microparticles can be flexibly and easily implemented using microfluidic lithography or micromolding-based particle fabrication techniques (Jang et al., 2023; Truong Hoang et al., 2024). This graphical encoding strategy enables large multiplexing capacity (up to 10^6) and simple decoding capability via deep learning-aided algorithms (Birtwell and Morgan, 2009; Choi et al., 2023). The nanoporous and water-like environment of hydrogel materials enables the dense functionalization of detection probes and efficient diffusion of reactants in the particles, which leads to enhanced detection signal and sensitivity (Le Goff et al., 2015; Song et al., 2023). Especially, by adding bioinert porogen into the precursor, such as polyethylene glycol (PEG), a mesoporous hydrogel structure can be implemented in the synthesized particles by size-exclusion effect during the free-radical polymerization (Choi et al., 2012). Thereby, biomolecules with high molecular weight (above 10 kDa), such as cell-free DNA, can easily react with the detection probes inside the particles through facilitated diffusion. However, even though the graphically encoded hydrogel microparticle has been utilized for detecting epigenetic markers, such as histone modification (Yeom et al., 2016), the multiplexed analysis for DNA methylation has not been investigated. Moreover, even though several encoded hydrogel microparticle-based RCA assays have been developed (Al Sulaiman et al., 2022; Mun et al., 2023), corresponding approaches were tailored to the detection of microRNA and SNPs, for which the detection process and clinical implications are different from DNA methylation.

In this study, we developed a graphically encoded hydrogel microparticle-based multiplexed detection platform for DNA methylation via streamlined integration of bisulfite conversion (BC), ligation-detection reaction (LDR), and hydrogel-based RCA. After incubation of the padlock DNA, which has complementary sequences against methylated DNA, with the BC-treated DNA products, the padlock DNA is ligated when hybridized with methylated target DNA. The ligated padlock DNA is then attached to the probe DNA in the encoded hydrogel particles and RCA-based fluorescence signal amplification is continued. Based on the development and optimization of this assay, methylated DNA can be quantitatively detected with femtomolar sensitivity. Furthermore, a low proportion of methylated DNA (down to 0.1 %) can be detected in a DNA mixture composed of methylated and unmethylated DNA. Finally, the methylation levels of VIM and SDC2 in DNA extracted from normal and colorectal cancer cell lines were determined, revealing the diagnostic potential of the developed assay for colorectal cancer.

2. Materials and methods

The materials and protocols for the fabrication of DNA probe-loaded particles, DNA methylation detection, DNA extraction from cell lines, particle imaging, and statistical analysis are included in the Supplementary Data. The nucleic acid sequences used are listed in Table S1.

3. Results and discussion

3.1. Development and optimization of hydrogel-based multiplexed DNA methylation detection

The overall DNA methylation detection process using the encoded

hydrogel microparticles is shown in Fig. 1. The first step of the assay is the BC process, in which unmethylated DNA cytosines are specifically converted to uracil, whereas methylated cytosines remain intact. Then, the BC-treated DNAs are incubated with T4 DNA ligases and padlock DNA, the sequences of which were fully complementary to those of the methylated target genes. In this study, we selected two target genes, vimentin (VIM) and SDC2, which are representative methylation markers for colorectal cancer (Han et al., 2019; Liu et al., 2017). After incubation, the padlock DNA hybridized with methylated DNA can be specifically ligated because T4 DNA ligase favors a double-stranded DNA (dsDNA) state (Mun et al., 2023).

After ligation, the circularized padlock DNA is hybridized to DNA probes functionalized with the encoded hydrogel microparticles. Hybridization conditions, such as reaction temperature and salt concentration, were selected according to previous hydrogel-based nucleic acid sensing studies (Jang et al., 2021; Mun et al., 2023; Song et al., 2023). The RCA reaction is then conducted from the duplex DNA composed of padlock DNA and DNA probes in the particles, mediated by phi29 DNA polymerases and dNTPs. Using RCA, the concatemer product is generated, and fluorescence labeling is implemented with sequential labeling of biotinylated DNA and streptavidin conjugated with R-phycoerythrin (SA-PE). Owing to the multiple labeling of SA-PE in a single concatemer originating from a single padlock DNA, a highly amplified fluorescence signal can be achieved. This streamlined assay procedure is technically distinct from previous hydrogel-based RCA assays (Al Sulaiman et al., 2022; Mun et al., 2023). For example, conventional assays do not require any pretreatment of the target nucleic acids, such as bisulfite conversion, because the corresponding assays target genetics rather than epigenetics.

To validate the assay, it was performed in the presence or absence of each essential component, including the methylated VIM target, T4 DNA ligase, phi29 DNA polymerase, and dNTPs (Fig. 2A). Consequently, the detection signal for the presence of all components was significantly higher than that in the other cases, indicating that each component, including the target DNA, was critical for implementing a successful assay. To validate the specific expression of the fluorescence signal for methylated DNA targets, we compared the detection signals between samples for the negative control, the unmethylated VIM target, and the methylated VIM target (positive control) (Fig. 2B). As a result, a remarkable detection signal was observed only in the presence of the methylated target, validating the feasibility and high specificity of the developed assay. The particle images below the graph for each case also supported the specificity of the developed DNA methylation detection technology (Fig. 2B). To inhibit non-specific ligation of padlock DNA and hybridization in the particles for mismatched dsDNA, the MutS enzyme was added to the reaction mixture, as MutS can bind to mismatched dsDNA and inhibit non-specific ligation and hybridization (Lee et al., 2022; Mishra et al., 2021). MutS is critically involved in the process of DNA repair, in which it binds to a mismatched site in double-stranded DNA with high specificity (Li, 2008). Considering this phenomenon, multiple nucleic acid sensing technologies have used MutS as a specificity enhancer, particularly for mutation discrimination (Lee et al., 2022; Mishra et al., 2021; Mun et al., 2023). The main principle for enhancing the detection specificity of MutS in the RCA process is the inhibition of undesired ligation of padlock DNA by impeding ligase activity (Lee et al., 2022; Mun et al., 2023). If a mismatch exists near the end of the padlock DNA, the ligase cannot efficiently link the ends of the padlock DNA because MutS occupies the mismatch site. The overall procedure for the preparation of DNA probe-modified hydrogel microparticles is illustrated in Fig. S1. The bright-field particle images used for detecting VIM and SDC2 in this study are presented in Fig. S2.

Padlock DNA is a crucial component of the assay because the amount of ligated padlock DNA hybridized with DNA probes in the particles is proportional to the detection signal of the assay. To determine the optimal concentration of padlock DNA for ligation, different samples were assayed by varying the concentration of padlock DNA (Fig. 2C). For the optimization process, 1xTE buffer spiked with 5 pM of the methylated VIM target was used. The signal-to-noise ratio (SNR), which is the ratio between the control-subtracted detection signal of a target presence case and the standard deviation of a control signal, was utilized for screening because it is a highly efficient tool for optimizing detection sensitivity (Jang et al., 2024). Consequently, the highest SNR was observed for a padlock DNA concentration of 10 nM. The presence of a peak in the optimization results can be explained by two factors. When the concentration of padlock DNA was too low, the amount of padlock DNA capable of ligation decreased, leading to a reduction in the detection signal due to the low amounts of RCA products in the hydrogel particles. However, when the padlock DNA concentration is too high, nonspecific interactions between the unligated padlock DNA and DNA probes in the particles inhibit the RCA process. Considering that phi29 DNA polymerase favors nick-free DNA complexes, the partial sequence complementarity between the unligated padlock DNA and the DNA probe in the particles can induce non-specific hybridization, interfering with the desired hybridization of the ligated padlock DNA.

Increased thermodynamic instability between the primer and DNA template due to several factors, such as mismatch, can alter the efficacy of polymerase-based DNA amplification (Boyle et al., 2009). PEG is

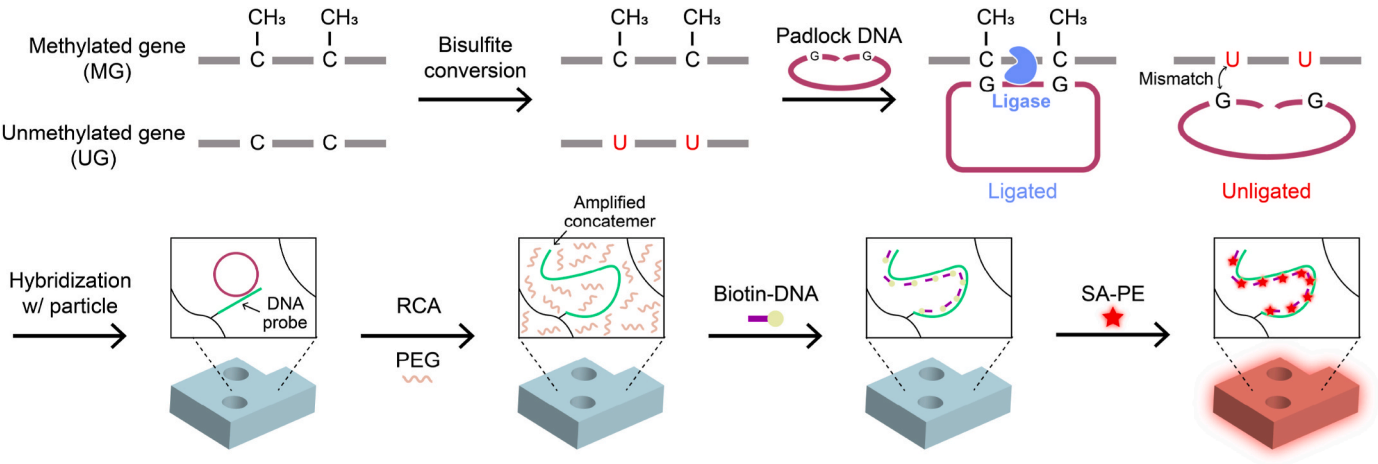

Fig. 1. Schematic of encoded hydrogel microparticle-based detection of DNA methylation. The assay procedures are composed of the three main steps; 1) bisulfite conversion (BC)-based sequence conversion of the DNA target, 2) ligation of the padlock DNA in the hybridized state with the methylated target, and 3) hydrogel-based RCA and fluorophore labeling after the hybridization of the ligated padlock DNA to the DNA probes in the particles.

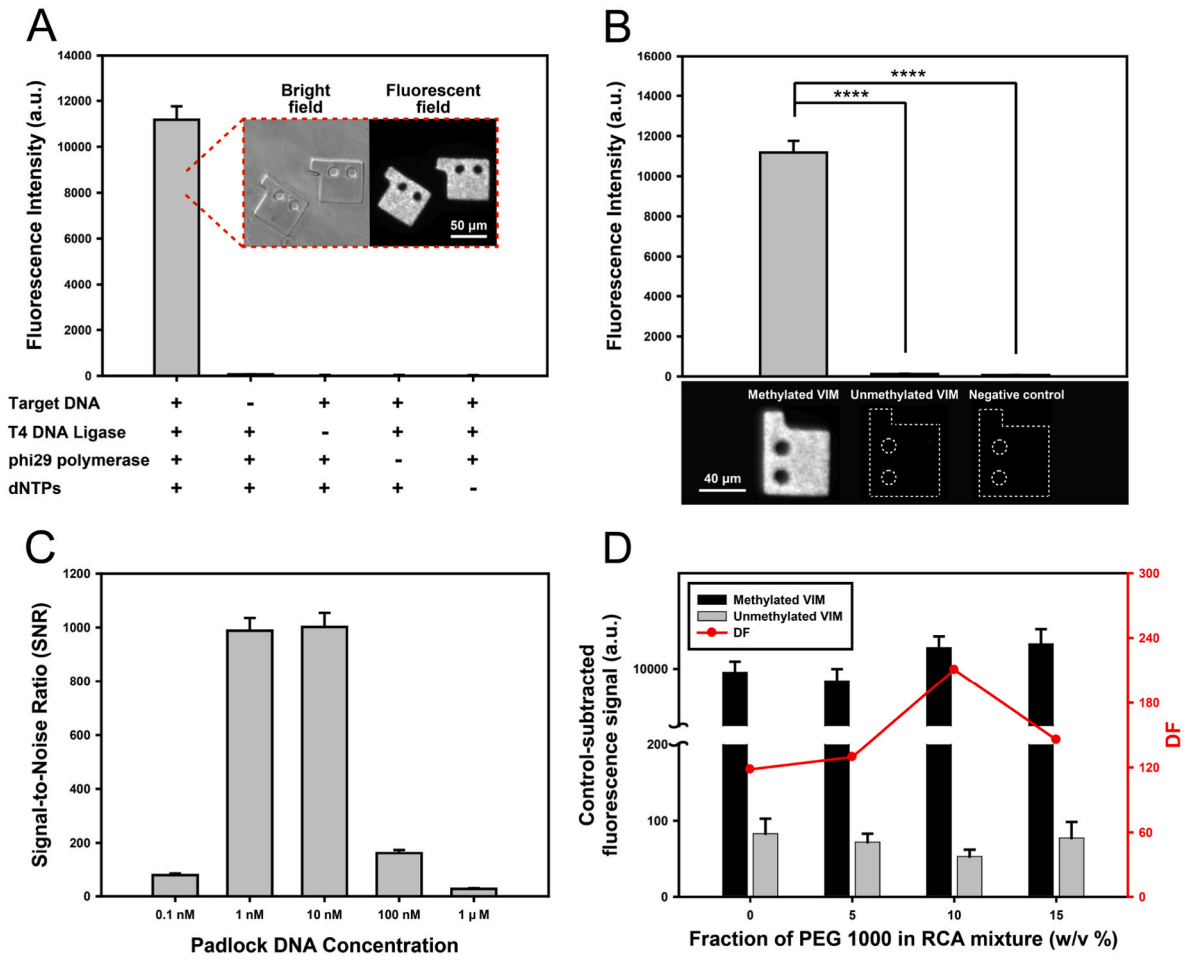

Fig. 2. A) Assay validation according to the presence or absence of each component, including the methylated VIM target, T4 DNA ligase, phi29 DNA polymerase, and dNTPs. Bright-field and fluorescent images present the particles after the assay had progressed with all components. B) Quantitative detection signal and particle images after the assay of methylated VIM target, unmethylated VIM target, and negative control (****$p < 0.0001$, $n = 11$). C) Optimization of padlock DNA concentration in the padlock DNA ligation process in terms of SNR. D) Optimization of PEG concentration in the RCA process in terms of discrimination factor (DF).

known to induce thermodynamic instability between two complementary DNAs through several mechanisms, such as altering the flexibility of secondary structures and the hydration state (Gu et al., 2013; Knowles et al., 2011). In particular, when a sequence mismatch exists in dsDNA, the destabilization effect can be more pronounced than in the case of a perfect match (Moon et al., 2022). Based on this phenomenon, our group utilized PEG additives in the RCA process to specifically discriminate SNPs in the previous study (Mun et al., 2023). PEG included in the RCA process can destabilize dsDNA composed of a DNA probe and padlock DNA containing a mismatch, thereby reducing non-specific ligation. Considering the specificity enhancement effect of PEG, we investigated whether PEG could enhance the specificity of DNA methylation. Among the diverse molecular weights, 1000 Da was selected for the PEG additives, considering that the precipitation of PEG frequently occurs in high-molecular weight cases. Four different concentrations (0 %, 5 %, 10 %, and 15 %) were screened by evaluating the discrimination factor (DF), which is the ratio between the control-subtracted signal for the methylated VIM target and that for the unmethylated target after assaying with the VIM-targeted probe and padlock DNA (Fig. 2D). Consequently, the enhancement of the DF by the addition of PEG was confirmed. In particular, the DF was highest when 10 % PEG 1000 was added. The decrease in DF for the 15 % sample may be attributed to the precipitation of PEG in the RCA mixture, which may lead to non-specific signal expression via the interaction of the precipitates with the polymer networks in the particles. In the 15 % case, increased turbidity of the samples was observed owing to the precipitates induced by the high amount of PEG additives. These precipitates can inhibit the efficient molecular diffusion of the reactants during RCA. In conclusion, we used 10 nM padlock DNA and 10 % PEG 1000 in the ligation and RCA processes for further experiments. We also confirmed the capability of robust and specific DNA methylation detection of SDC2, another target gene (Fig. S3). Furthermore, we detected DNA methylation for VIM (5 pM) and SDC2 (100 pM) by spiking these targets into fetal bovine serum (FBS) to investigate whether DNA methylation could be directly detected in complex media (Fig. S4). Consequently, analogous to the detection results for the buffer samples (1xTET with 50 mM NaCl) in Fig. 2B, a remarkably high detection signal for only the methylated target was observed for VIM and SDC2. In addition, the DFs of VIM and SDC2 in the FBS-based assay were 340.5 and 136.2, respectively, which were comparable to the buffer-based assay results (Fig. 2D).

To investigate whether the methylation of other CpG sites interfered with site-specific methylation detection, we utilized the target DNAs without BC treatment as a model for globally methylated DNA, considering that the methylated CpG site after BC treatment was identical to the unmethylated CpG site without BC treatment in terms of sequence. We detected VIM and SDC2 targets without the BC process and compared the detection signals with those of BC-based assays. As shown in Fig. S5, the detection signal for the BC-free model targets was comparable (deviation within 20 %) to that of the BC-based assays for both VIM and SDC2. Furthermore, the detection signals for unmethylated targets and negative controls for VIM (Fig. 2B) and SDC2 (Fig. S3) in the BC-based assays were remarkably lower than those for methylated

targets in the BC-free assays. These results indicate that globally induced DNA methylation did not significantly interfere with site-specific methylation detection.

3.2. Characterization of the detection performance for DNA methylation

Considering the limited amount of DNA in biological samples, especially in easily collected samples, such as stool samples, high detection sensitivity is required for clinical application of the assay. Thus, to investigate the sensitivity and capability for quantitative detection, we plotted calibration curves for different concentrations of VIM and SDC2 targets (Fig. 3A and B). For both targets, linear regression (R^2 for VIM and SDC2:0.9806 and 0.9979, respectively) was observed, validating the quantitative detectability of the developed assay. To calculate the limit of detection (LoD) of the assay, we derived the concentration values corresponding to three times the standard deviation of the control signals in each calibration curve. As a result, the LoD for VIM and SDC2 genes were revealed as 23.3 fM and 54.1 fM, respectively. In addition, we calculated the limit of quantification (LoQ) by deriving the concentration values corresponding to 10 times the standard deviation of the control signals to clarify the possible range for quantifying the target concentrations. The LoQ for VIM and SDC2 genes were revealed as 75.4 fM and 157 fM, respectively.

The ability to detect slight levels of DNA methylation in total DNA is important for the accurate prediction and early diagnosis of cancer. Thus, multiple samples with diverse compositions of methylated and unmethylated targets were assayed for the VIM and SDC2 targets (Fig. 3C and D). To calculate the minimum proportion for differentiating the methylated targets in the mixture, we derived the LoD for the methylation level, which corresponded to three times the standard deviation of the signal for the sample containing only unmethylated targets in the regression line of the curves. 10 pM VIM and 100 pM SDC2 were used for the analysis, considering the consistency in the amount of detection signal between each target, referring to the singleplex calibration curve (Fig. 3A and B). Consequently, 0.1 % and 0.2 % of the methylated targets could be differentiated from the unmethylated targets for VIM and SDC2, respectively, indicating the high specificity of the developed assay. The LoQs in the methylation specificity analysis were 0.5 % and 0.7 % for VIM and SDC2, respectively. To compare the detection performance of the developed DNA methylation detection assay with other technologies, we have added Table S2 in the supplementary data, which extensively compares the multiplexing capacity, sensitivity, specificity, assay time, and complexity with other technologies. As presented in Table S2, the LoD values for detectable and differentiable DNA methylation levels of the developed assay were comparable or superior to those of previous studies addressing the detection of DNA methylation, even with a graphical encoding-based high multiplexing capability. In particular, the superior ability to differentiate low methylation levels can be attributed to the high antifouling capability of the PEG materials of the particles and the specific RCA process triggered by the ligation of padlock DNA in the presence of a methylated gene (Chen et al., 2019b; Lee et al., 2022; Mun et al., 2023). The reproducibility of the assay was validated by conducting five independent assays for VIM targets and characterizing batch-to-batch

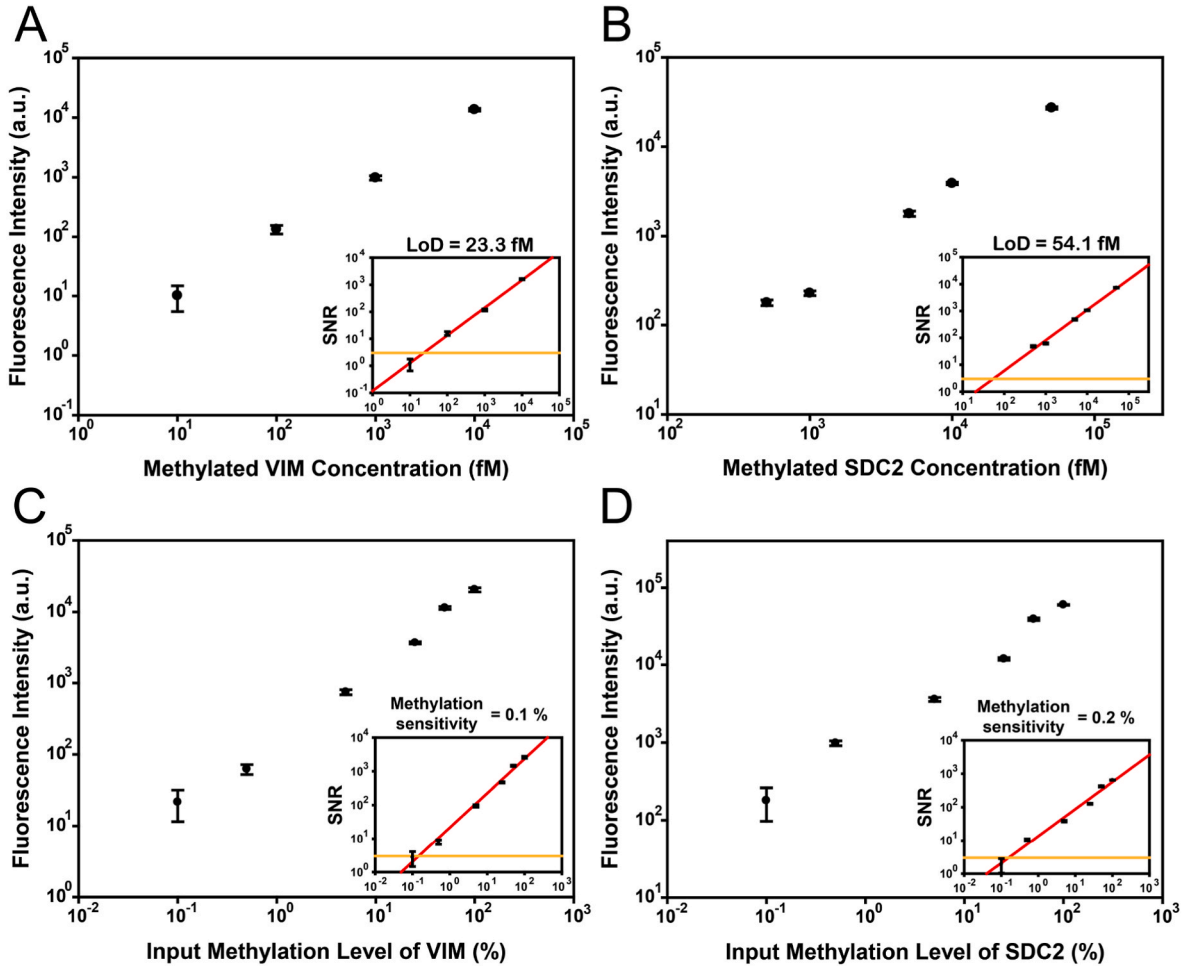

Fig. 3. Calibration curve between detection signal and methylated target DNA concentration for VIM (A) and SDC2 (B). Calibration curve for VIM (C) and SDC2 (D) between detection signal and the proportion of methylated DNA in total DNA.

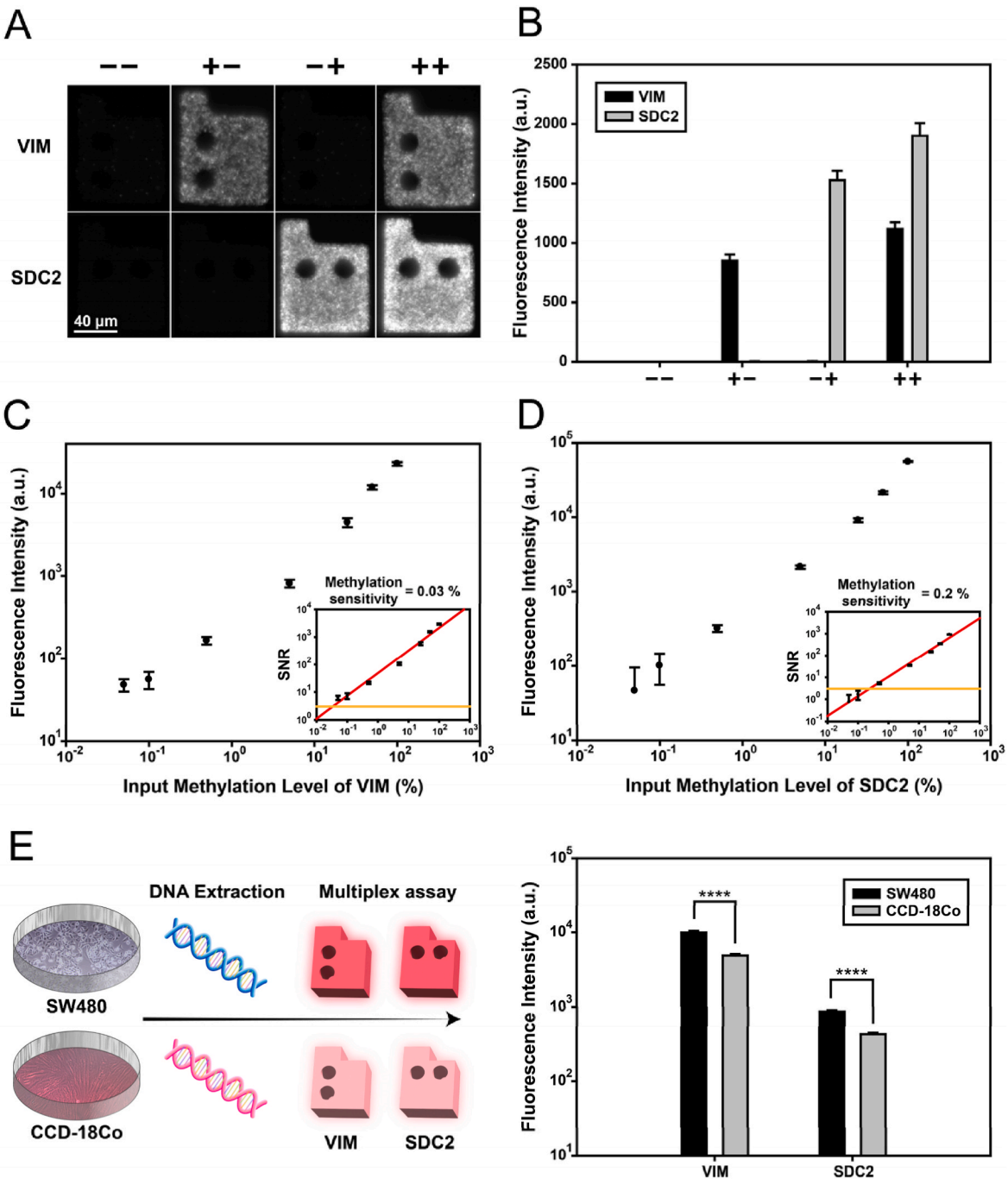

Fig. 4. Multiplexed detection for VIM and SDC2. A) The fluorescent particle images after assaying four combination samples. The symbols of plus (+) and minus (−) represent the presence and absence of each target in the samples, respectively. B) The quantitative analysis of the detection signal for VIM and SDC2 from four combination samples. The calibration curve for VIM (C) and SDC2 (D) between the detection signal and the proportion of methylated DNA in total DNA for the multiplexed assay. E) Encoded hydrogel microparticle-based duplex methylation detection of VIM and SDC2 genes in DNA extracted from SW480 and CCD-18Co cell lines (****$p < 0.0001$, $n = 19$).

signal variation (Fig. S6). Consequently, the coefficient of variation (CV) for each sample was 5.6 %, indicating the robustness of the developed assay.

3.3. Multiplexed DNA methylation detection for VIM and SDC2

To investigate the multiplexing capability of the developed DNA methylation sensing technique, we first conducted a duplex assay for samples containing the artificial target DNAs. Four combinations of samples were assayed in the presence or absence of VIM and SDC2. As shown in Fig. 4A–B, the fluorescence of particles for each target type was significantly expressed only when the target was present in the samples. The detection signal for target presence was consistent for each target type, indicating the robustness and reproducibility of the multiplexed assay. Additionally, in the absence of the target, non-specific signal expression was negligible, indicating superior specificity of the developed assay. To investigate the compatibility between the singleplex and multiplex assays, the recovery rate was calculated (Jang et al., 2024). First, the target concentration was calculated by comparing the detection signal of the multiplexed assay to that of the calibration curve. The

obtained target concentration was divided by the theoretical spiked-in target concentration. The recovery rates for VIM and SDC2 were 81.9 % and 94.7 %, respectively (Table S3). Considering that practically acceptable recovery rates range between 70 % and 130 % (Djoba Siawaya et al., 2008), the recovery rate analysis validates the consistency between the singleplex and multiplex assays.

To explore whether the capability to differentiate methylated genes was still valid in the multiplexed assay, we conducted a calibration analysis between the detection signal and the proportion of methylated DNA in the total DNA for VIM and SDC2 (Fig. 4C–D). Analysis of the capability of differentiating methylated genes in total DNA in the multiplex assay was conducted by serial dilution of the sample containing both VIM and SDC2 targets, the methylation proportion of which was adjusted to be identical for each target (Snellenberg et al., 2012). 0.5 pM VIM and 5 pM SDC2 were used for multiplexed analysis of methylation sensitivity. We selected the corresponding low target concentrations for multiplexing because validation of the detection specificity for low target concentrations in a multiplexed assay is important for conducting multiplexed DNA methylation detection in biological samples, such as cell lysates (Fig. 4E). For each target, the LoD values for DNA methylation differentiation were found to be 0.03 % and 0.2 %, indicating the ability to differentiate trace amounts of methylated genes in total DNA, even in the multiplexed assay. The ratio of sensitivity between VIM and SDC2 was approximately 7, which was not negligible. Sensitivity variability at this level is commonly observed in multiplexed nucleic acid detection (Al Sulaiman et al., 2022; Mun et al., 2023). Because of sequence heterogeneity, each target had a different melting temperature and GC content. Therefore, the detection performance can vary in multiplexed detection, where the detection conditions (e.g., incubation temperature) are unified. We expect that the synchronization of detection performance can be implemented by further refining the sequence design of functional nucleic acids, such as padlock DNA and DNA probes. The LoQ values for methylation sensitivity in the multiplexed assay were 0.1 % and 0.9 % for VIM and SDC2, respectively.

As shown in Figs. 3B–4C, the x-axis values of the lowest data points were higher than the LoD values. Several biosensing studies, including hydrogel microparticle-based assays, have selected data points above LoD values in calibration analysis to derive the LoD (Al Sulaiman et al., 2022; Mun et al., 2023; Wang et al., 2022; Zhang et al., 2025). In addition, as shown in Figs. 3B–4C, the lowest data points and LoD values were within an order of magnitude, which is an acceptable level based on previous studies.

Finally, to confirm whether the developed assay could be adapted to real biological samples, we extracted DNA from a colorectal cancer cell line (SW 480) and a normal colon cell line (CCD-18Co) to compare methylation levels. After preparing the samples with the same concentration of DNA for each cell line (8 ng/μL), multiplexed DNA methylation sensing was conducted (Fig. 4E). Consequently, for both targets, a significantly higher methylation level ($p < 0.0001$) was observed, which is consistent with clinical results (Han et al., 2019; Liu et al., 2017). This result indicates that the developed assay can be applied to biological samples, such as cell lysates for DNA methylation analysis.

Compared to other encoding strategies in suspension microarrays (e.g., fluorescence and photonic crystals), graphically encoded microparticle-based bioassays have superior multiplexing capability owing to the negligible interference between code information. For fluorescence- and photonic crystal-based encoding strategies, the issue of spectral overlapping reduces the multiplexing capability and induces vulnerability to misinterpretation of code information in a multiplex assay (Jet et al., 2021). In contrast, graphically encoded particles can be easily decoded with high accuracy (>99 %) using an automatic analysis system, such as a machine learning (ML) model (Choi et al., 2023). This graphical encoding strategy retains a theoretical multiplexing capacity of up to 10^6 (Birtwell and Morgan, 2009). Thus, based on the design of the particle geometry and sequence for the padlock DNA and DNA probes, the multiplexing capability of the system is expected to be scalable by over an order of magnitude (Fig. S7).

In terms of cost, the developed hydrogel microparticle-based bioassay is advantageous because it utilizes only 50 particles with a picoliter volume for each target in a single assay. In addition, based on the multiplexing capability, the consumption of reagents, such as DNA polymerase for a single target, can be significantly reduced. The simultaneous analysis of 10 gene targets can be achieved at a cost of less than $20 using the developed assay platform.

4. Conclusion

In this study, we developed a multiplexed DNA methylation detection platform that integrated bisulfite-based sequence conversion, padlock DNA ligation, and hydrogel-based RCA. The developed assay avoids complex pre-amplification steps, such as PCR, and establishes a streamlined process based on the first adoption of a graphically encoding-based suspension microarray platform in the field of DNA methylation detection. Using this assay, two types of colorectal cancer genes (VIM and SDC2) were quantitatively detected with double-digit femtomolar sensitivity. In particular, this assay can differentiate a very low portion of DNA methylation (down to 0.1 %) in total DNA, which potentiates the early diagnosis of cancer without invasive diagnostic approaches, such as endoscopy and tissue biopsy. The multiplexing capability of colorectal cancer markers was validated with negligible non-specific signal expression and a robust recovery rate acceptable for practical applications (between 70 % and 130 %). Based on robust sensitivity and specificity, different DNA methylation levels for VIM and SDC2 were successfully observed between colorectal cancer cells (SW480) and normal colon cells (CCD-18Co), indicating the adaptability of the presented assay to actual biological samples. Furthermore, we validated that the developed assay can be adapted not only to extracted DNA samples, but also to complex biological media (e.g., serum), potentiating DNA methylation detection directly from complex media without a cumbersome DNA extraction process. The developed assay has certain limitations, including a long assay time (more than 8 h), redundant assays, and particle rinsing steps. However, the adoption of several approaches can help address these issues. For example, the integration of RCA and padlock DNA hybridization into a single step, based on the compatibility of the reaction conditions, can reduce the total assay time and number of steps. Furthermore, the use of a label-free fluorescence expression system, such as G-quadruplex-based thioflavin intercalation, can also be useful for reducing the entire assay time and number of steps without requiring additional fluorophore labeling. Even though two types of targets were used to validate the multiplexing capability in this research, it is expected that the number of multiplexes can be further increased by the flexible design of particle codes and nucleic acid sequences, such as the DNA probe and padlock DNA. Graphical encoding-based multiplexing capabilities can lead to comprehensive DNA methylation analysis and multi-cancer diagnosis. In addition, the application of the developed assay can be further extended to the methylomics field by investigating the relationship between DNA methylation levels and diverse epigenetic factors, such as aging, stress, and pathogenesis.

CRediT authorship contribution statement

Wookyoung Jang: Writing – review & editing, Writing – original draft, Methodology, Investigation, Conceptualization. **So Jung Oh:** Writing – review & editing, Writing – original draft, Visualization, Validation, Methodology, Data curation. **Eun Sun Kim:** Writing – review & editing, Writing – original draft, Resources, Project administration, Methodology. **Ki Wan Bong:** Writing – review & editing, Writing – original draft, Visualization, Supervision, Project administration, Methodology, Funding acquisition, Conceptualization.

Declaration of competing interest

The authors declare that they have no known competing financial interests or personal relationships that could have appeared to influence the work reported in this paper.

Acknowledgements

The National Research Foundation (NRF) grant supported the research with funding from the Korean government (MSIT, RS-2024-00456113) and the Korean government (MSIT, RS-2025-02263336). Also, the Technology Innovation Program (Development of Superfast Multiplex Technology for the Examination of Diagnosis of Infectious Disease and in-Body Response Test, 20018111) supported this work with funding from the Ministry of Trade, Industry and Energy (MOTIE, Korea).

Appendix A. Supplementary data

Supplementary data to this article can be found online at https://doi.org/10.1016/j.bios.2025.117725.

Data availability

Data will be made available on request.

References

Al Sulaiman, D., Juthani, N., Doyle, P.S., 2022. Adv. Healthcare Mater. 11, e2102332. https://doi.org/10.1002/adhm.202102332.
Ballestar, E., Sawalha, A.H., Lu, Q., 2020. Nat. Rev. Rheumatol. 16, 514–524. https://doi.org/10.1038/s41584-020-0470-9.
Bautista-Sánchez, D., Arriaga-Canon, C., Pedroza-Torres, A., De La Rosa-Velázquez, I.A., González-Barrios, R., Contreras-Espinosa, L., Montiel-Manríquez, Rogelio, Castro-Hernández, C., Fragoso-Ontiveros, V., Álvarez-Gómez, R.M., Herrera, L.A., 2020. Mol. Ther. Nucleic Acids 20, 409–420. https://doi.org/10.1016/j.omtn.2020.03.003.
Bibikova, M., Barnes, B., Tsan, C., Ho, V., Klotzle, B., Le, J.M., Delano, D., Zhang, L., Schroth, G.P., Gunderson, K.L., Fan, J.B., Shen, R., 2011. Genomics 98, 288–295. https://doi.org/10.1016/j.ygeno.2011.07.007.
Bibikova, M., Lin, Z., Zhou, L., Chudin, E., Garcia, E.W., Wu, B., Doucet, D., Thomas, N.J., Wang, Y., Vollmer, E., Goldmann, T., Seifart, C., Jiang, W., Barker, D.L., Chee, M.S., Floros, J., Fan, J.B., 2006. Genome Res. 16, 383–393. https://doi.org/10.1101/gr.4410706.
Birtwell, S., Morgan, H., 2009. Integr. Biol. 1, 345–362. https://doi.org/10.1039/b905502a.
Boyle, B., Dallaire, N., MacKay, J., 2009. BMC Biotechnol. 9, 1–15. https://doi.org/10.1186/1472-6750-9-75.
Chen, J., Sun, H., Tang, W., Zhou, L., Xie, X., Qu, Z., Chen, M., Wang, S., Yang, T., Dai, Y., Wang, Y., Gao, T., Zhou, Q., Song, Z., Liao, M., Liu, W., 2019a. J. Cancer 10, 5264–5271. https://doi.org/10.7150/jca.34944.
Chen, Q., Yu, S., Zhang, D., Zhang, W., Zhang, H., Zou, J., Mao, Z., Yuan, Y., Gao, C., Liu, R., 2019b. J. Am. Chem. Soc. 141, 16772–16780. https://doi.org/10.1021/jacs.9b07105.
Chen, X., Zhang, J., Ruan, W., Huang, M., Wang, C., Wang, H., Jiang, Z., Wang, S., Liu, Z., Liu, C., Tan, W., Yang, J., Chen, J., Chen, Z., Li, X., Zhang, X., Xu, P., Chen, L., Xie, R., Zhou, Q., Xu, S., Irwin, D.L., Fan, J.B., Huang, J., Lin, T., 2020. J. Clin. Investig. 130, 6278–6289. https://doi.org/10.1172/JCI139597.
Choi, J.H., Jang, W., Lim, Y.J., Mun, S.J., Bong, K.W., 2023. ACS Sens. 8, 3158–3166. https://doi.org/10.1021/acssensors.3c00857.
Choi, N.W., Kim, J., Chapin, S.C., Duong, T., Donohue, E., Pandey, P., Broom, W., Hill, W.A., Doyle, P.S., 2012. Anal. Chem. 84, 9370–9378. https://doi.org/10.1021/ac302128u.
Choi, W., Park, E., Bae, S., Choi, K.H., Han, S., Son, K.H., Lee, D.Y., Cho, I.J., Seong, H., Hwang, K.S., Nam, J.M., Choi, J., Lee, H., Choi, N., 2022. Small 18, e2105538. https://doi.org/10.1002/smll.202105538.
Djoba Siawaya, J.F., Roberts, T., Babb, C., Black, G., Golakai, H.J., Stanley, K., Bapela, N. B., Hoal, E., Parida, S., van Helden, P., Walzl, G., 2008. PLoS One 3, e2535. https://doi.org/10.1371/journal.pone.0002535.
Gong, T., Borgard, H., Zhang, Z., Chen, S., Gao, Z., Deng, Y., 2022. Small Methods 6, e2101251. https://doi.org/10.1002/smtd.202101251.
Gu, X., Nguyen, M.T., Overacre, A., Seaton, S., Schroeder, S.J., 2013. J. Phys. Chem. B 117, 3531–3540. https://doi.org/10.1021/jp312154d.
Han, Y.D., Oh, T.J., Chung, T.H., Jang, H.W., Kim, Y.N., An, S., Kim, N.K., 2019. Clin. Epigenet. 11, 51. https://doi.org/10.1186/s13148-019-0642-0.
Healy, B., Khan, A., Metezai, H., Blyth, I., Asad, H., 2021. Clin. Med. 21, e54–e56. https://doi.org/10.7861/clinmed.2020-0839.
Heiss, J.A., Just, A.C., 2018. Clin. Epigenet. 10, 73. https://doi.org/10.1186/s13148-018-0504-1.
Jang, W., Kim, J., Mun, S.J., Kim, S.M., Bong, K.W., 2021. Biomedicines 9, 848. https://doi.org/10.3390/biomedicines9070848.
Jang, W., Mun, S.J., Kim, S.Y., Bong, K.W., 2023. Colloid Surf. B-Biointerfaces 222, 113088. https://doi.org/10.1016/j.colsurfb.2022.113088.
Jang, W., Song, E.L., Mun, S.J., Bong, K.W., 2024. Biosens. Bioelectron. 261, 116465. https://doi.org/10.1016/j.bios.2024.116465.
Jet, T., Gines, G., Rondelez, Y., Taly, V., 2021. Chem. Soc. Rev. 50, 4141–4161. https://doi.org/10.1039/d0cs00609b.
Jiang, M., Zhang, Y., Fei, J., Chang, X., Fan, W., Qian, X., Zhang, T., Lu, D., 2010. Lab. Invest. 90, 282–290. https://doi.org/10.1038/labinvest.2009.132.
Jin, Z., Liu, Y., 2018. Genes Dis 5, 1–8. https://doi.org/10.1016/j.gendis.2018.01.002.
Kim, J., Shim, J.S., Han, B.H., Kim, H.J., Park, J., Cho, I.J., Kang, S.G., Kang, J.Y., Bong, K.W., Choi, N., 2021. Biosens. Bioelectron. 192, 113504. https://doi.org/10.1016/j.bios.2021.113504.
Knowles, D.B., LaCroix, A.S., Deines, N.F., Shkel, I., Record Jr., M.T., 2011. Proc. Natl. Acad. Sci. U. S. A. 108, 12699–12704. https://doi.org/10.1073/pnas.1103382108.
Le Goff, G.C., Srinivas, R.L., Hill, W.A., Doyle, P.S., 2015. Eur. Polym. J. 72, 386–412. https://doi.org/10.1016/j.eurpolymj.2015.02.022.
Lee, S., You, J., Baek, I., Park, H., Jang, K., Park, C., Na, S., 2022. Biosens. Bioelectron. 210, 114295. https://doi.org/10.1016/j.bios.2022.114295.
Li, G.M., 2008. Cell Res. 18, 85–98. https://doi.org/10.1038/cr.2007.115.
Li, H., Huang, J., Lv, J., An, H., Zhang, X., Zhang, Z., Fan, C., Hu, J., 2005. Angew. Chem.-Int. Edit. 44, 5100–5103. https://doi.org/10.1002/anie.200500403.
Li, H., Xie, Y., Chen, F., Bai, H., Xiu, L., Zhou, X., Guo, X., Hu, Q., Yin, K., 2023a. Chem. Soc. Rev. 52, 361–382. https://doi.org/10.1039/d2cs00594h.
Li, Y., Liu, Y., Tang, X., Qiao, J., Kou, J., Man, S., Zhu, L., Ma, L., 2023b. ACS Sens. 8, 4420–4441. https://doi.org/10.1021/acssensors.3c01463.
Liang, N., Li, B., Jia, Z., Wang, C., Wu, P., Zheng, T., Wang, Y., Qiu, F., Wu, Y., Su, J., 2021. Nat. Biomed. Eng. 5, 586–599. https://doi.org/10.1038/s41551-021-00746-5.
Liu, Y., Wu, H., Zhou, Q., Song, Q., Rui, J., Zou, B., Zhou, G., 2017. Biosens. Bioelectron. 92, 596–601. https://doi.org/10.1016/j.bios.2016.10.054.
Mishra, S., Jeon, J., Kang, J.K., Song, S.H., Kim, T.Y., Ban, C., Choi, H., Kim, Y., Kim, M., Park, J.W., 2021. Nano Lett. 21, 9061–9068. https://doi.org/10.1021/acs.nanolett.1c02728.
Moon, H.J., Mun, S.J., Lee, J.H., Roh, Y.H., Lim, Y.J., Bong, K.W., 2022. Talanta 245, 123480. https://doi.org/10.1016/j.talanta.2022.123480.
Mun, S.J., Jang, W., Park, H.S., Lim, Y.J., Yang, T.J., Bong, K.W., 2023. Biosens. Bioelectron. 241, 115670. https://doi.org/10.1016/j.bios.2023.115670.
Schumacher, A., Kapranov, P., Kaminsky, Z., Flanagan, J., Assadzadeh, A., Yau, P., Virtanen, C., Winegarden, N., Cheng, J., Gingeras, T., Petronis, A., 2006. Nucleic Acids Res. 34, 528–542. https://doi.org/10.1093/nar/gkj461.
Snellenberg, S., De Strooper, L.M.A., Hesselink, A.T., Meijer, C.J.L.M., Snijders, P.J.F., Heideman, D.A.M., Steenbergen, R.D.M., 2012. BMC Cancer 12, 1–9. https://doi.org/10.1186/1471-2407-12-551.
Song, C.W., Bae, S.H., Bong, K.W., Han, C.S., 2023. Sens. Actuator B-Chem. 380, 133376. https://doi.org/10.1016/j.snb.2023.133376.
Suzuki, M.M., Bird, A., 2008. Nat. Rev. Genet. 9, 465–476. https://doi.org/10.1038/nrg2341.
Truong Hoang, Q., Kim, D.Y., Park, H.S., Jang, W., Nguyen Cao, T.G., Kang, J.H., Ko, Y. T., Mun, S.J., Bhang, S.H., Shim, M.S., 2024. Adv. Funct. Mater. 34, 2306078. https://doi.org/10.1002/adfm.202306078.
Wang, C., Wu, J., Huang, H., Xu, Q., Ju, H., 2022. Anal. Chem. 94, 15695–15702. https://doi.org/10.1021/acs.analchem.2c02934.
Wani, K., Aldape, K.D., 2016. Methods Mol. Biol. 1392, 177–186. https://doi.org/10.1007/978-1-4939-3360-0_16.
Weng, Y.L., An, R., Shin, J., Song, H., Ming, G.L., 2013. Neurotherapeutics 10, 556–567. https://doi.org/10.1007/s13311-013-0223-4.
Wu, C., Dougan, T.J., Walt, D.R., 2022. ACS Nano 16, 1025–1035. https://doi.org/10.1021/acsnano.1c08675.
Yeom, S.Y., Son, C.H., Kim, B.S., Tag, S.H., Nam, E., Shin, H., Kim, S.H., Gang, H., Lee, H. J., Choi, J., Im, H.I., Cho, I.J., Choi, N., 2016. Anal. Chem. 88, 4259–4268. https://doi.org/10.1021/acs.analchem.5b04190.
Yu, X., Zhao, H., Wang, R., Chen, Y., Ouyang, X., Li, W., Sun, Y., Peng, A., 2024. Cell Death Discov. 10, 28. https://doi.org/10.1038/s41420-024-01803-z.
Zhang, J., Kang, M., Li, J., Huang, B., Lu, K., Abudula, A., Wen, H., Guan, G., 2025. Anal. Chim. Acta 1358, 344088. https://doi.org/10.1016/j.aca.2025.344088.
Zhang, L., Wang, D., Li, Z., Lin, G., Li, J., Zhang, R., 2024. iScience 27, 111177. https://doi.org/10.1016/j.isci.2024.111177.
Zhao, Y., O'Keefe, C.M., Hsieh, K., Cope, L., Joyce, S.C., Pisanic, T.R., Herman, J.G., Wang, T.H., 2023. Adv. Sci. 10, e2206518. https://doi.org/10.1002/advs.202206518.